Available online at www.sciencedirect.com
SCIENCE DIRECT®
Proceedings of the Combustion Institute 30 (2005) 2613–2621
Proceedings of the Combustion Institute
www.elsevier.com/locate/proci

Investigations of the scaling criteria for a mild combustion burner

Sudarshan Kumar, P.J. Paul*, H.S. Mukunda

Combustion Gasification and Propulsion Laboratory, Department of Aerospace Engineering, Indian Institute of Science, Bangalore 560 012, India

Abstract

In this paper, a new strategy for scaling burners based on "mild combustion" is evolved and adopted to scaling a burner from 3 to a 150 kW burner at a high heat release rate of 5 MW/m^3. Existing scaling methods (constant velocity, constant residence time, and Cole's procedure [Proc. Combust. Inst. 28 (2000) 1297]) are found to be inadequate for mild combustion burners. Constant velocity approach leads to reduced heat release rates at large sizes and constant residence time approach in unacceptable levels of pressure drop across the system. To achieve mild combustion at high heat release rates at all scales, a modified approach with high recirculation is adopted in the present studies. Major geometrical dimensions are scaled as $D \sim Q^{1/3}$ with an air injection velocity of ~100 m/s ($\Delta p \sim 600$ mm water gauge). Using CFD support, the position of air injection holes is selected to enhance the recirculation rates. The precise role of secondary air is to increase the recirculation rates and burn up the residual CO in the downstream. Measurements of temperature and oxidizer concentrations inside 3 kW, 150 kW burner and a jet flame are used to distinguish the combustion process in these burners. The burner can be used for a wide range of fuels from LPG to producer gas as extremes. Up to 8 dB of noise level reduction is observed in comparison to the conventional combustion mode. Exhaust NO emissions below 26 and 3 ppm and temperatures 1710 and 1520 K were measured for LPG and producer gas when the burner is operated at stoichiometry.

Keywords: Flameless combustion; Mild combustion; Burner scaling; NO_x emissions

1. Introduction

Guidelines for scaling are important in the design of combustion systems. A large number of dimensionless groups for scaling are proposed by Spalding [1] and Beer and Chigier [2]. It is recognized that maintaining all the variables constant during the process is not possible partly because of internal inconsistencies. It is imperative to adapt scaling based on a selected set of non-dimensional quantities.

Constant velocity, CV and constant residence time, CRT approaches have been applied to scale up the burners and furnaces from laboratory scale [3–10]. For a burner, the total thermal input is given as $Q = \dot{m}_f H = K\rho U_o D_o^2$. In CV approach, the burner inlet velocity is maintained constant, and geometrical dimensions are derived from the relationship $D_2/D_1 = (Q_2/Q_1)^{1/2}$. For CRT approach, the ratio D_o/U_o (inertial or convective timescale) is maintained constant while increasing the burner thermal input. The new physical dimensions are determined through a relationship $D_2/D_1 = (Q_2/$

* Corresponding author. Fax: +91 80 236 016 92.
E-mail address: paul@cgpl.iisc.ernet.in (P.J. Paul).

1540-7489/$ - see front matter © 2004 The Combustion Institute. Published by Elsevier Inc. All rights reserved.
doi:10.1016/j.proci.2004.07.045

Nomenclature

CRT	Constant residence time scaling approach	Q, Q_1, Q_2	Burner thermal input (kW)
CV	Constant velocity scaling approach	U_o, U_a, U_f	Inlet velocity of air/fuel or characteristic velocity (m/s)
D, D_o, D_1, D_2	Different burner dimensions	$\dot{m}_a$, $\dot{m}_f$	Air and fuel flow rates
f_v	Volume fraction	$\dot{Q}'''$	Heat release rate per unit volume MW /m^3
H	Calorific value of fuel	ρ	Density of air/fuel (kg/m^3)
LPG	Liquefied petroleum gas (~80% butane and 20% propane)	τ_{mixing}, τ_a, τ_f	Characteristic mixing time or convective timescales, D_o/U_o (ls)
Producer gas	Low calorific value gas (H_2 ~ 20%, CO ~ 20%, CH_4 ~ 2%, CO_2 ~ 13% and rest N_2)		

$Q_1)^{1/3}$. In another approach adopted by Cole et al. [8], both air velocity and jet area are increased equally for scaling combustors. The velocity and jet diameters are scaled as $U_2/U_1 = (Q_2/Q_1)^{1/2}$ and $D_2/D_1 = (Q_2/Q_1)^{1/4}$ to burner inputs. More details about the variation of critical parameters with different scaling approaches are given in Table 1.

It is known that CV approach increases the characteristic mixing time and reduces the rate of mixing [3–10]. To maintain constant rate of mixing, the inlet velocity should be increased as $Q^{1/3}$ with burner thermal input [4–6,8]. In Cole's [8] approach, jet velocity increases at faster rate than jet diameter. Therefore, both CRT and Cole's [8] approaches lead to large pressure drop across the combustion system. The experimental investigations using Cole's [8] approach on an acoustically excited combustor showed consistent performance for pollutant emissions, flame stability, and enhanced mixing at smaller levels. The improvement in emissions' performance at larger power scales is reported to be insignificant.

The scaling studies on swirl stabilized pulverized coal burners have shown that NO_x emissions depend on local fluid flow behavior in the internal recirculation zone [4,5]. Computational investigations by Weber and Breussin [6] predicted that beyond a certain thermal input, NO_x emissions remained independent of the scaling approach used.

CV approach fails to produce aerodynamic similarity in the near burner region for swirl stabilized natural gas burners [7]. This is a critical factor for NO_x formation in the gas burners. Detailed analysis of NO_x emissions from two gas burners at 67 and 266 kW thermal levels showed the importance of prompt NO formation in the near burner zone of a combustion system [10].

The exhaust gas recirculation for NO_x reduction from combustion systems has drawn interest due to its promising features [11–16]. When recirculation rates are high enough and at temperatures greater than the auto-ignition temperature of the fuel, a stable combustion mode exists. This combustion mode is known as mild or flameless

Table 1
Comparison of various parameters in different scaling approaches

Scaling approaches	Geometric scaling $D = (D_2/D_1)$	Velocity scaling $U = (U_2/U_1)$	τ_{mixing}	Re	$\dot{Q}'''$
CV	$\sim Q^{1/2}$	Constant	$\sim Q^{1/2}$	$\sim Q^{1/2}$	$\sim Q^{-1/2}$
CRT	$\sim Q^{1/3}$	$\sim Q^{1/3}$	Constant	$\sim Q^{2/3}$	Constant
Cole [9]	$\sim Q^{1/4}$	$\sim Q^{1/2}$	$\sim Q^{-1/4}$	$\sim Q^{3/4}$	$\sim Q^{1/4}$
Present	$\sim Q^{1/3}$	~100 m/s	$\sim Q^{1/3}$	$\sim Q^{1/3}$	Constant

Table 2
Summary of the previous work in mild combustion and residence times used in these experiments

Ref.	U_f (m/s)	τ_f (μs)	U_a (m/s)	τ_a (μs)	$\dot{Q}'''$ $(MW/m3)$	Q (kW)
[12]	20	250	73.7	74.6	0.32	10
[13]	9.34	503.2	33	151.51	0.18	6
[14]	12.57	318.21	28.9	162.58	0.18	6
[18]	100	100	70	1771	0.023	580
[20]	7.9–70.7	114–4.2	—	—	—	—
[15]	20–100	25–5	26–130	77–15.5	5.6	1–5
Present	243	3	95	52	5.6	150

combustion [11–19]. Table 2 summarizes the work carried out on mild combustion. Lower convective timescales seem to be a critical factor to achieve mild combustion with high $\dot{Q}'''$ (~5 MW/m^3) and reactants at ambient temperature. The previous experiments are conducted in the thermal range of 1–580 kW with low heat release rates (23–320 kW/m^3) [12–15].

To scale a burner with high $\dot{Q}'''$, if one uses a CRT method, jet velocity increases as $Q^{1/3}$ and hence leads to unacceptable levels of pressure drop across the system beyond a certain thermal input range as shown in Table 3. One needs to explore other alternatives to scale a mild combustion burner while maintaining the geometric, dynamic, and thermal similarities.

The objectives of the current research are to use the results of 3 kW laboratory scale burner, scale it to a large level, in this case 150 kW, establish mild combustion in a high heat release burner, and suggest scaling laws for the mild combustors.

2. Computations

The objectives of the computational studies are to optimize the burner geometry, to quantify the recirculation rates and to predict the combustion and fluid flow behavior of a 150 kW mild combustion burner. The same code that was used for 3 kW laboratory burner is used here. The details related to computational strategy, fluid flow, and combustion modeling of the burner can be found in Sudarshan et al. [15]. Since the geometry presents a sixfold symmetry with six alternate fuel and air injection jet arrangements along the central axis, one-sixth part of the burner is considered for the numerical simulation. To obtain grid independent results, grid resolution studies are carried out with the number of grid points varying from 100,000 to 1,000,000. The results with respect to 600,000 grid points were within 1% for all meshes up to 1,000,000 grid points.

3. Geometry optimization and computational results

The 3 kW laboratory burner investigated earlier by Sudarshan et al. [15] is scaled using CV, CRT, and Cole's [8] scaling principles. Table 3 shows the detailed dimensions, velocities, and other related details of the 150 kW scaled burner with different approaches. The burner is theoretically scaled to 2 MW to show the effect of different approaches on recirculation rates and heat release rates. Figure 1 shows the effect of different scaling approaches on physical geometry of 150 kW burner. The physical dimensions of the scaled burner decrease from CV to CRT and Cole's [8] approach, and corresponding $\dot{Q}'''$ increases. Figure 2 shows the variation of recirculation rates in 150 kW scaled burner with different scaling approaches obtained from computational studies. Curve (a) shows that

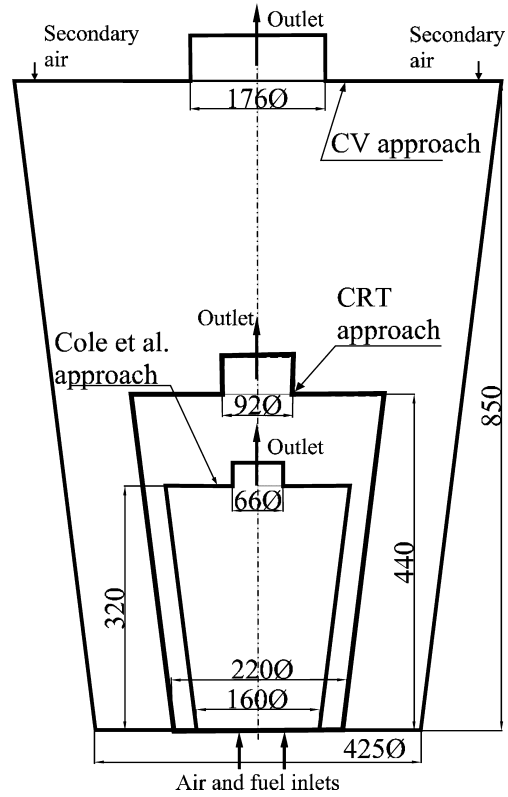

Fig. 1. Details of the 150 kW scaled burner using different approaches.

Table 3
Summary of the geometrical dimensions with different scaling approaches

Scale factor	1	10	50	667
Q (kW)	3	30	150	2000
D_a, U_a for CRT	2, 80	4.3, 172	7.4, 291	17.5, 698
D_1, D_2, L (mm) for CRT	60, 90, 120	130, 194, 258	221, 331, 440	525, 790, 1050
D_1, D_2, L (mm) for CV	60, 90, 120	190, 285 380	425, 636, 850	1550, 2325, 3100
D_1, D_2, L (mm) Cole [8]	60, 90, 120	107, 160, 214	160, 240, 320	305, 458, 610
Present D_a, U_a	2, 80	—	5, 95	—
Present τ_a (μs)	25	—	52.4	—
Recirculation rate	2.8	—	2.3	—

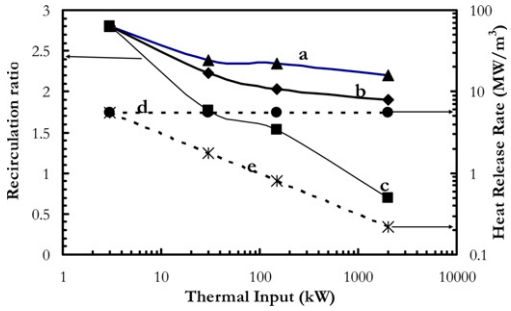

Fig. 2. Variation of recirculation rate and heat release rates with thermal power. Curve (a) Recirculation rate variation with CRT approach. Curve (b) Recirculation rate variation with CV approach. Curve (c) Recirculation rate variation when major burner dimensions are determined through $D \sim Q^{1/3}$ with an air injection velocity of 100 m/s. Curve (d) Variation of heat release rate for CRT approach. Curve (e) Variation of heat release rate for CV approach.

the recirculation rates drop from 280% to 220% as the burner is scaled from 3 kW level to 2 MW using CRT approach. The air inlet velocity (scaled as $U_o \sim Q^{1/3}$) increases from 79 to 698 m/s. This leads to unacceptable level of pressure drop across the combustion systems. Curve (d) shows that corresponding heat release rate remains constant with CRT approach. Similarly Cole's [8] ($U_o \sim Q^{1/2}$) approach also results in large pressure drop across the combustion systems.

When CV scaling approach is used to determine the burner dimensions, the recirculation rates drop from 280% to 190% as shown by curve (b). Curve (e) represents the corresponding $\dot{Q}'''$ variation with CV approach. The heat release rates drastically drop as $1/Q^{1/2}$ from 5.6 to 0.217 MW/m^3 as burner is scaled from 3 kW to 2 MW. Curve (c) represents variation of recirculation rates in the burner when the major burner dimensions are determined to maintain high $\dot{Q}'''$ at 5.6 MW/m^3 and air inlet velocity at ~100 m/s, an affordable choice in industrial applications. To maintain $\dot{Q}'''$ constant, combustion system volume should be increased in proportion to thermal input. Therefore, major burner dimensions are scaled as $D \sim Q^{1/3}$. In the current scaling strategy, recirculation rates drop to 153% at 150 kW and 70% at 2 MW level, thus making it difficult to achieve mild combustion in the scaled burners.

At this point of time, a 150 kW burner scaled from 3 kW laboratory burner is tested experimentally for the demonstration of mild combustion mode. The major dimensions are determined using $D \sim Q^{1/3}$ to maintain high $\dot{Q}'''$. Air jet velocities of 100 m/s are considered. This experimental burner is tested with both LPG and producer gas (typical producer gas composition CO 20%, H_2 20%, CO_2 13%, CH_4 2%, and rest N_2). It is observed that due to low recirculation rates and large air and fuel jet diameters (large convective timescales of air and fuel jets), the combustion zones are clearly visible as a kind of highly confined jet flames attached to either air or fuel jets (for detailed operating conditions see Table 4). Overall observed emission levels are low. The presence of highly confined jet flames in the combustion zone prompted further investigations.

The steep reduction in recirculation rates led to the exploration of other alternatives to increase the overall recirculation rates to achieve mild combustion. Initial trials with different injection schemes showed that various air/fuel injection schemes had very little effect on overall recirculation rates. The air and fuel injection details are shown in Fig. 3. Both air and fuel are injected as a set of six holes at different locations at 90 mm pitch diameter. The diameters and number of air and fuel jets are estimated to keep the D_o/U_o ratio in the same range as for laboratory scale burner operational range (see Table 4). The recirculation rates are further enhanced by appropriately optimizing the position of secondary air injection (~20% of total air). The secondary air is injected as a set of multiple high-speed jets from the top. A number of calculations are carried out to reveal the effect of location and velocity of secondary air injection on recirculation rates. Figure 4 shows the variation of the recirculation rate with the position of secondary air with respect to the

Table 4
Summary of experiments carried out on the mild combustion burners (MC-mild combustion, AF-attached flames, and PG-Producer gas)

Burner	Q (kW)	U_f (m/s)	D_f (mm)	τ_f (μs)	U_a (m/s)	D_a (mm)	τ_a (μs)	Fuel	Remarks
I	1	20	0.5	25	27	2	74	LPG	MC
	3	60	0.5	8.3	80	2	25	LPG	MC
	5	100	0.5	5	135	2	14.8	LPG	MC
II	150	125	2	16	100	10	100	LPG	AF
	150	95	12	126	128	10	78	PG	AF
	150	63	6	95	78	5	64	PG	AF
	150	92	5	54	78	5	64	PG	MC
	150	243	0.7	2.9	95	5	52.4	LPG	MC

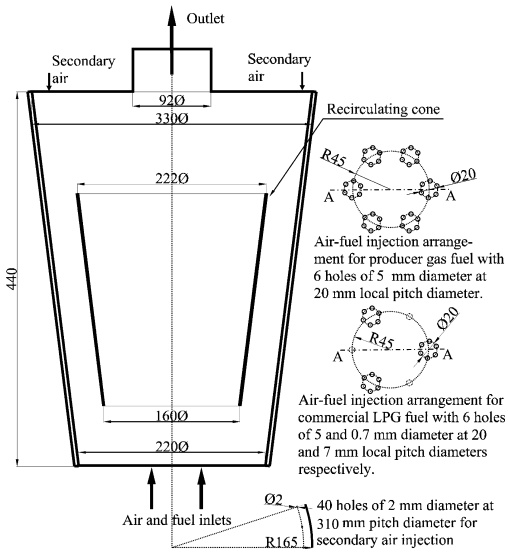

Fig. 3. Details of optimized configuration for 150 kW burner with alternate peripheral injection schemes for both LPG and producer gas fuels.

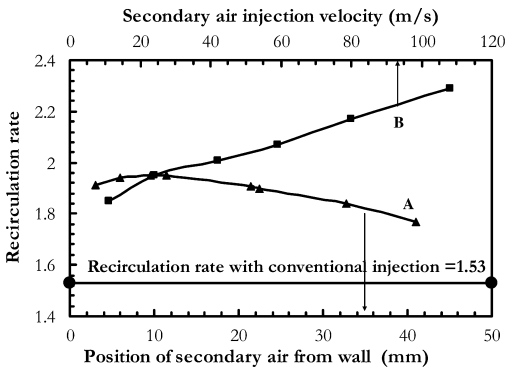

Fig. 4. Variation of recirculation rate with secondary air position and velocity. Curve (A) Variation of recirculation rate with secondary air injection position. Curve (B) Variation of recirculation rate with secondary air velocity at optimum position.

wall and secondary air velocity. Curve (a) shows that the position of secondary jets has a strong effect on the recirculation rate. The recirculation rate reaches a maximum of 196% for a constant injection velocity of 24 m/s when injection holes are located at 11 mm from the wall. Curve (b) shows that recirculation rate varies almost linearly with the secondary injection velocity. Compared to the conventionally injected secondary air [15] at 150 kW level, the recirculation rates are enhanced by ~80%.

To establish a quantitative comparison between the burners at different scales, temperature–volume and O_2–volume behavior is extracted from the calculations. The volume elements for $\Delta T = 100$ K and $\Delta X_{O_2} = 0.01$ steps are determined over the entire combustor and plotted for (a) a turbulent jet diffusion flames (b) 150 kW optimized burner, and (c) 3 kW laboratory burner. Figures 5 and 6 show the cumulative distribution of volume fraction variation with temperature and O_2 for burners at different scales. For a turbulent jet flame, $f_v = 0.54$ for temperature <1000 K and $f_v = 0.54$ for O_2 mass fraction >0.15. For 150 kW optimized burner, $f_v = 0.93$ for temperature >1000 K (autoignition temperature of the fuel) and is almost uniformly distributed over the whole range. Similarly, $f_v = 0.96$ for O_2 mass fraction <0.15 and is uniformly distributed in the range of 0–0.15. For a 3 kW mild combustion burner, $f_v = 0.93$ for temperature >1300 K and for O_2 mass fraction <0.07, $f_v = 0.97$. This deviation of temperature and oxidizer mass fraction distributions from 3 kW mild combustion burner [15] appears significant. This is attributed to the fact that in the current burner, the number of air-fuel jets is six times larger than the previously investigated 3 kW burner. The group

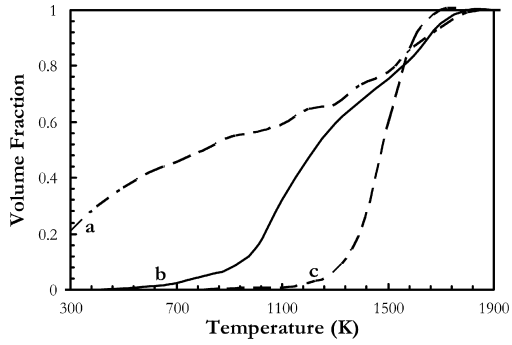

Fig. 5. Predicted cumulative temperature–volume behavior for (a) classical turbulent jet flame. (b) 150 kW scaled burner. (c) 3 kW laboratory scale burner.

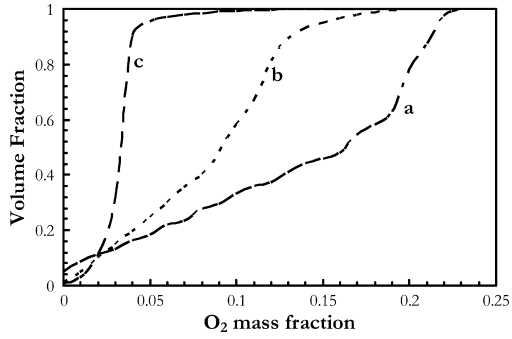

Fig. 6. Predicted cumulative O_2–volume behavior for (a) classical turbulent jet flame. (b) 150 kW scaled burner. (c) 3 kW laboratory scale burner.

of air jets influenced a large volume when compared to a single air jet. For the mild combustion mode, O_2 is typically in the range of 0–0.15, and temperature is greater than 1000 K (auto-ignition temperature of the fuel) [17]. Hence, even case (b) can be considered as in mild combustion mode.

4. Scaling of mild combustion burners

Table 4 shows the summary of convective timescales for different combinations of air and fuel jets employed during the experimental investigations. Highly confined, attached, and fluctuating jet flames appeared in the combustion zone below 1 kW. The reduction in the air and fuel flow rates leads to reduction in recirculation rates and results in the appearance of attached flames within the reaction zone. At this operating condition, convective timescales for air and fuel jets are 74 and 25 μs, respectively.

At 150 kW thermal level, experiments are carried out with different air-fuel injection combinations for both LPG and producer gas. Highly confined jet flames are observed visibly, attached to either air or fuel jets for the cases of convective timescales greater than ~80 μs. It is observed that mild combustion is obtained successfully with both LPG and producer gas for D_o/U_o ratio below 80 μs. From a series of experiments in the 1–150 kW range on mild combustion burners, it is concluded that for successful scaling of mild combustion burners with high heat release rates, D_o/U_o ratio should be maintained below ~80 μs.

Mild combustion is achieved when flames are lifted off from the primary burner zone at high velocities. This can be explained on the basis of lift-off concept of simple jet diffusion flames, which depends on local temperature, reactant concentration, velocity, and diameter of the injection jets. Confined jet flames are expected to appear in the combustion zone as long the velocities are below blow-off and recirculation rates are low.

5. Experiments

Two fuels are selected for the experimental studies on 150 kW burner to show that the burner can be used over a wide range of fuels. Producer gas and LPG are chosen as extremes (Calorific value variation 4.5–45 MJ/kg). The burner is operated at stoichiometry with 150 kW thermal input. The dimensions of the burner are fixed by the total thermal input and $\dot{Q}'''$ in the burner. These dimensions are further modified through a number of computations aimed at optimizing the burner configuration. The details of the air and fuel injection schemes for LPG and producer gas are shown in Fig. 3. Typical air and LPG mass flow rates are 50 and 3.2 g/s. The flow rates for producer gas and air are 39 and 47 g/s. Eighty percentage of the total air is supplied through the primary inlet and 20% through the secondary inlets. The temperatures in the reaction zone are measured by using 50 μm Pt-13%Pt-Rh thermocouples. Measured temperatures are corrected for heat loss by radiation. The corrected temperatures are accurate within ±50 K of actual temperature. Species (NO, CO, CO_2, and O_2) concentrations are measured in the reaction zone by using Quintox KM-9106 flue gas analyzer. A specially designed water-cooled stainless steel probe is used to draw the sample gases from the reaction zone. The sample gases are immediately cooled, dried, and then transferred to the analyzer continuously. A Lutron SL-4001 sound level meter is used to measure the sound levels during the combustion experiments. More details of the Quintox gas analyzer and sound level meter are mentioned in Sudarshan et al. [15]. The noise level measurements are taken at a point 50 mm from outlet of the burner at the same plane.

6. Results and discussion

Most of the results presented in this section are for the 150 kW case. The burner is operated at a stoichiometric air/fuel ratio. Figure 7 shows the distinction between the conventional combustion and mild combustion operation at 150 kW level with LPG and producer gas. The conventional combustion mode is achieved by reducing the air and fuel flow rates in the system leading to lower recirculation rates and shifts in operation to attached flame mode as in Fig. 7A. The burner operation in mild combustion mode is shown in Fig. 7B–D. The injection arrangement is clearly visible and totally transparent at the injection plane. A very weak flame is present in the reaction zone which is light bluish in color and barely visible. All the walls are red hot and glowing consistently. This combustion mode is achieved by large recirculation rates of the combustion products into the fresh reactants.

The acoustic level measurements are carried out during the cold flow (only air jets), mild combustion mode, and conventional combustion mode. The measured levels are 103, 105, and 113 dB, respectively. Approximately 8 dB of noise reduction is observed when operational mode shifts from conventional combustion to mild combustion for reasons known earlier [15]. Similar noise reduction is observed when the burner is operated with producer gas.

The composition of species is measured at two axial locations, 150 and 400 mm downstream from the injection plane. Figure 8 shows the CO, CO_2, and O_2 mole fractions and temperatures measured at 150 mm axial position across section

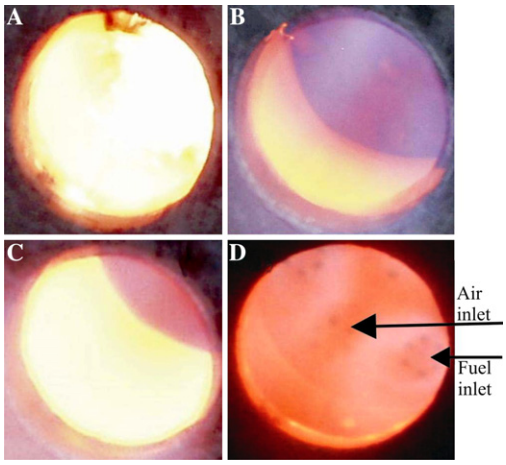

Fig. 7. Comparison between conventional and mild combustion. (A) Conventional turbulent combustion with low recirculation rates. (B,C) Mild combustion mode with LPG fuel. (D) Mild combustion mode with producer gas fuel.

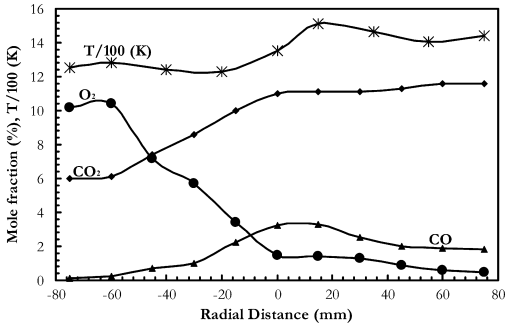

Fig. 8. Species concentration and temperature measurements with LPG fuel at 150 mm from injection plane.

A–A (Fig. 3). O_2 mole fraction drops from 10% on air jet side to very low values of 1% on fuel jet side. O_2 is fairly well distributed with small gradients across the measuring plane. Measured O_2 mole fraction clearly indicates the air and fuel jet injection sides (across section A–A). The species composition variation across this plane is moderately small. Low species gradients, high temperature, and low concentration of reacting species suggest the presence of a slow reaction over a large area. The measured temperature varies in the range of 1200–1550 K and fairly uniform over the reaction zone.

Figure 9 shows the species and temperature measurements 400 mm downstream. The temperatures are far more uniform and vary between 1500 and 1750 K. The temperature gradients at this plane are much smaller than those compared to 150 mm. The species concentration variation at this plane is very small. The uniformity in species

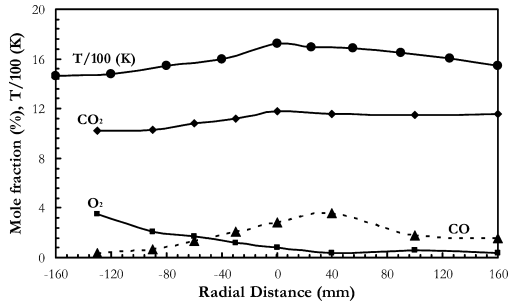

Fig. 9. Species compositions and temperature measurements with LPG fuel at 400 mm from injection plane.

composition across the plane suggests at the continuance of slow combustion reaction at this plane. At exhaust, the emissions recorded are 26 ppm NO, 1% CO, and an average temperature 1710 K. The CO emissions are in the range of previously reported experiments [15]. It is observed during the experiments that very low CO emissions (~0.03%) are recorded when ~10% more air is added downstream to dilute the combustion products and burn the residual CO.

The injection plane of the burner is slightly modified to operate the same burner with producer gas (calorific value ~4.5 MJ/kg) as shown in Fig. 3B. The typical stoichiometric ratio for producer gas is ~1.2. A 200 kW thermal level woody biomass-based gasifier continuously supplied producer gas for burner operation [21,22]. Figure 10 shows the species and temperature measurements at 400 mm across section A–A. The temperatures measured at 400 mm are quite uniform across the radial plane. The important point to note is that temperature is much more uniform in the reaction zone than compared to the LPG fuel. Temperature variations across the radial plane are less than 200 K, and mean temperature is above 1400 K. The average temperature measured across the exhaust plane is 1520 K. Large concentrations of O_2 on one side and CO on the other side indicate the approximate position of the air and fuel jets.

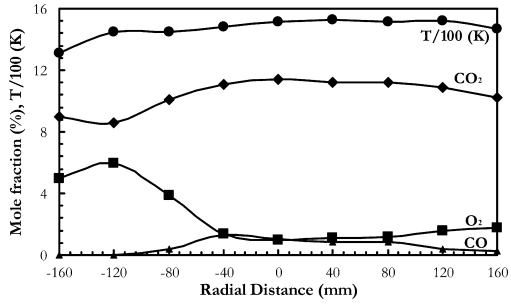

Fig. 10. Species concentration and temperature measurements with producer gas fuel at 400 mm from injection point.

Small gradients of CO, CO_2, and O_2 describe the distributive and sluggish nature of reaction zone over a large area. Similar behavior of species concentration and temperatures are recorded at 150 mm from the injection plane. In contrast to the LPG operated burner, the NO emissions from producer gas operation are very low. The measured CO and NO emissions at the exhaust are 0.211% and 3 ppm against the 1% and 26 ppm for LPG. The difference in emissions could be attributed to a difference in the average operating temperature (~200 K) and in calorific values of two fuels.

7. Summary

The proposed scaling approach is shown to be successful in scaling a 3 kW laboratory scale mild combustion burner to 150 kW level. The scaled burner is operated with two different fuels and shown to achieve mild combustion at high release rates (~5.6 MW/m^3) with both air and fuel at ambient temperature. The design of its features has been achieved and optimized through preliminary computations, which helped in revealing the effect of secondary air position and injection velocity on the recirculation rate. Recirculation rate is enhanced from 153% to 230% by appropriately positioning the secondary air injection. The distribution of temperature and O_2 mass fraction in the combustion chamber is essential in the mild combustion regime. The cumulative behavior of temperature–volume and O_2–volume distributions show that O_2 mass fraction is <0.15 in 96% of the total volume, and temperature is >1000 K in 93% of the total volume. The presence of low O_2 mass fraction and high temperature zone in most of the combustion chamber volume is indicative of mild combustion at larger power levels with current approach. Scaling of air and fuel jet combination based on convective timescales (maintaining below 80 μs) is an interesting observation. It needs to be explored further based on simple jet flame experiments in the similar conditions that exist in mild combustion burners.

The experiments with LPG and producer gas recorded exhaust emissions of NO below 26 and 3 ppm, respectively. The CO exhaust emissions observed are 1% and 0.221% with heat release rates ~5.6 MW/m^3. The measured temperature and O_2 gradients in radial direction are moderately small, which implies that combustion is taking place in mild combustion regime. The outstanding low chemical emissions, high heat release rates, operation with two fuels, and low acoustic emission features strongly indicate the potential for successful scaling to large power levels and use in industrial furnaces.

References

[1] D.B. Spalding, *Proc. Combust. Inst.* 9 (1962) 833–843.
[2] J.M. Beer, N.A. Chigier, *Combustion Aerodynamics.* Wiley Press, New York, 1972 (Chapter 7).
[3] R. Weber, *Proc. Combust Inst.* 26 (1996) 3343–3354.
[4] J.P. Smart, D.J. Morgan, P.A. Roberts, *Proc. Combust. Inst.* 24 (1992) 1365–1372.
[5] J.P. Smart, D.J. Morgan, *Combust. Sci. Technol.* 100 (1994) 331–343.
[6] R. Weber, F. Breussin, *Proc. Combust. Inst.* 27 (1998) 2957–2964.
[7] T.C.A. Hsieh, W.J.A. Dahm, J.F. Driscoll, *Combust. Flame.* 114 (1998) 54–80.
[8] J.A. Cole, T.P. Parr, N.C. Widmer, K.J. Wilson, K.C. Schadow, W.M.R. Seeker, *Proc. Combust. Inst.* 28 (2000) 1297–1304.
[9] M. Sadakata, Y. Hirose, *Fuel* 73 (8) (1994) 1338–1342.
[10] A.D. Al-Fawaz, J.T. Dearden, M. Hedley, J.T. Missaghi, M. Pourkashanian, A. Williams, L.T. Yap, *Proc. Combust. Inst.* 25 (1994) 1027–1034.
[11] J.A. Wunning, J.G. Wunning, *Prog. Energy Combust. Sci.* 23 (12) (1997) 81–94.
[12] T. Plessing, N. Peters, J.G. Wunning, *Proc. Combust. Inst.* 27 (1998) 3197–3204.
[13] B. Ozdemir, N. Peters, *Exper. Fluids* 30 (2001) 683–695.
[14] P.J. Coelho, N. Peters, *Combust. Flame* 123 (2001) 503–518.
[15] K. Sudarshan, P.J. Paul, H.S. Mukunda, *Proc. Combust. Inst.* 29 (2002) 1131–1137.
[16] M. de Joannon, G. Langella, F. Beretta, A. Cavaliere, C. Noviello, *Proc. Mediterr. Combust. Sympos.* 3 (1999) 347–360.
[17] A. Milani, A. Saponaro, *IFRF Combust. J. Article* 200101 (2001).
[18] R. Weber, S. Orsino, L. Nicolas, A. Verlaan, *Proc. Combust. Inst.* 28 (2000) 1315–1321.
[19] M. Mancini, R. Weber, U. Bollettini, *Proc. Combust. Inst.* 29 (2002) 1155–1164.
[20] S. Lille, T. Dobski, W. Blasiak, *J. Propuls. Power* 16 (4) (2000) 595–600.
[21] H.S. Mukunda, S. Dasappa, U. Shrinivasa, in: T.B. Johansson, H. Kelly (Eds.), *Renewable Energy–Sources for Fuels and Electricity.* Island Press, Washington, DC, 1993, pp. 699–728.
[22] ABETS, *Biomass to Energy—The Science and Technology of the IISc Bio-energy Systems.* ABETS, Indian Institute of Science Bangas, India.

Comments

Josette Bellan, Jet Propulsion Laboratory, USA. As you mentioned, Gutmark and Grinstein already performed some work on this topic. There are also studies in the literature on elliptic and triangular jets. We have performed ourselves 3-D DNS for single phase and two-phase flows with evaporating drops in circular,

elliptic, square, rectangular, and triangular geometries [1]. The consensus is that the presence of curvature induces a very large enhancement in stream-wise vorticity, and the flow in this direction overtaking the "core" flow produces the axis switching. Thus, this is the physics of axis switching, not the "overdoing" stated in the presentation. Moreover, elliptic, rectangular, and triangular geometries result in axis switching, but not square geometries, which only exhibit a 45° rotation [1,2]. Please comment.

References

[1] M. Abdel-Hameed, J. Bellan, *Phys. Fluids* 14 (10) (2002) 3655–3675.
[2] R.S. Miller, C.K. Madina, P. Givi, *Comput. Fluids* 24(1) (1995) 1.

Reply. Vortex dynamics, including axis switching, depends on the nonlinear interaction among all three vorticity components. The author does not believe that an enhanced streamwise vorticity alone provides the physics of axis switching, contrary to the comments made. The streamwise vorticity would not tell the difference between a major and a minor axes, nor the difference between a square or a rectangular jet. For example, the streamwise vortex pattern and strength would be the same, whether the initial minor axis is aligned with x-direction or y-direction, but the spreading rates in the two cases in a fixed direction (for example, x-direction) are completely different.

As discussed in the paper, the author believes that axis switching is due to the different magnitudes of the vorticity components along the major and minor axes, which led to different entrainment rates and spreading rates along the two axes. The differences are ultimately caused by the aspect ratio and curvature effects, which are configuration-dependent. The role of the streamwise vorticity is not to cause the differences in flow properties along the major and minor axes directly, but to influence the vorticity components along the two axis directions through vortex stretching. The reason why a square jet "rotates" only 45° is because the jet spreading takes place in a symmetric fashion in the 45°, 135°, 225°, and 315°-directions. Another such "rotation" would return it to the initial square position, so it does not seem to have undergone a 180° rotation (axis switching). The author believes that the present papers offer a more comprehensive explanation of axis switching than before.

●

Michael Delichatsios, University of Ulster, UK. In buoyant flames the velocity accelerates approximately as $Z^{1/2}$ so that the Reynolds number increases. Thus, more grid points are needed for DNS downstream than near the source to assure the same numerical accuracy. Have you estimated whether your chosen grid spacing is adequate throughout the field of your calculations?

Reply. As a DNS, the grid resolution was chosen to be sufficient throughout the computational domain. The final grids used were a result of extensive grid-independence tests. Adequacy of grid resolution was established by monitoring relevant quantities during a simulation and by checking key parameters in the final results.

●

G.S. Nathan, University of Adelaide, Australia. Your model assumed a uniform initial velocity profile. In a real fire, the initial velocity is determined by devolatilization, which in turn, depends on the heat transfer from the flame. It can be expected, therefore, that the real profile will be non-uniform, with the degree of non-uniformity increasing with aspect ratio. Please comment on the effect of these issues on your results.

Reply. The author agrees that non-uniformity of the initial conditions is an intrinsic feature of any real fire, which was not included in the study. However, such non-uniformity is expected to have a secondary, though important, effect on the results presented because the fire/flame dynamics considered here are mainly influenced by the source configuration.